Modeling of Flexible-Link Manipulators with Prismatic Joints

Rex J. Theodore and Ashitava Ghosal

Abstract—The axially translating flexible link in flexible manipulators with a prismatic joint can be modeled using the Euler–Bernoulli beam equation together with the convective terms. In general, the method of separation of variables cannot be applied to solve this partial differential equation. In this paper, we present a nondimensional form of the Euler–Bernoulli beam equation using the concept of group velocity and present conditions under which separation of variables and assumed modes method can be used. The use of clamped-mass boundary conditions lead to a time-dependent frequency equation for the translating flexible beam. We present a novel method to solve this time-dependent frequency equation by using a differential form of the frequency equation. We then present a systematic modeling procedure for spatial multi-link flexible manipulators having both revolute and prismatic joints. The assumed mode/Lagrangian formulation of dynamics is employed to derive closed form equations of motion. We show, using a model-based control law, that the closed-loop dynamic response of modal variables become unstable during retraction of a flexible link, compared to the stable dynamic response during extension of the link. Numerical simulation results are presented for a flexible spatial RRP configuration robot arm. We show that the numerical results compare favorably with those obtained by using a finite element-based model.

I. INTRODUCTION

Modeling and control of manipulators with flexible links having only revolute joints have been discussed extensively in the literature [1]–[6], while the research on modeling prismatic jointed flexible-link manipulators is limited [7]–[11]. When a link with the prismatic joint is modeled as flexible, the system becomes a moving boundary value problem. Moving boundary value problems have been considered in other context such as axially moving beam problems [12]–[14], and deployment dynamics of flexible spacecraft [15], [16].

Tabarrok *et al.* [13] studied the dynamics of an axially moving beam. They presented certain properties of the mode shapes of clamped-free beams inflexure, as the beam length varies with time. They also derived the equations of motion of a simple cantilever beam having an axial motion on a stationary rigid base by using Newton's second law. Buffinton and Kane [12] studied the dynamics of a beam moving at a prescribed rate over two bilateral supports. Regarding the supports as kinematical constraints imposed on an unrestrained beam, equations of motion were formulated by applying an alternative form of Kane's method [17] and using assumed modes technique to discretize the beam. Buffinton [7] later extended this formulation to investigate the motion characteristics of a planar RP elastic manipulator considering the translational member as a slender beam. Tsuchiya [16] studied the dynamics of a spacecraft during extension of flexible appendages under the assumption of small extension velocity. Extensive discussions about this assumption were madeby Jankovic [18].

In case of flexible-link manipulators with prismatic joints, the complexity ofthe dynamic model increases many fold as the length

of the vibrating link that translates, changes with time. Chalhoub and Ulsoy [8] investigated the interrelationship between the arm structural flexibility and a linear controller design of a spherical coordinate (RRP) robot arm. The equations of motion were derived by the assumed mode/Lagrangian approach with the last link considered as flexible. Wang and Wei [10] studied the vibration problem of a moving slender prismatic beam using a Galerkin approximation with time-dependent basis functions and by applying Newton's second law. Yuh and Young [11] presented the experimental results to validate the approximated dynamic model derived using assumed modes method for a flexible beam which has a rotational and translational motion.

In all the aforementioned works, it is invariably assumed that the translating flexible links can be modeled as beams in flexure with clamped-free boundary conditions, leading to a time-independent frequency equation [7], [12], [14]. The "free" boundary condition however may lead to inaccurate mode shapes and over-estimated eigen frequencies which may have destabilizing effect when the translating flexible robot link carries a payloador when a wrist is attached at distal end of the axially moving elastic beam [19]. In such cases the "clamped-mass" boundary conditions are more appropriate. Moreover, use of assumed modes method to discretize flexibility of a translating elastic link may not be valid, as the principle of separation of space-dependent eigenfunctions and time-dependent modal amplitudes is not valid under the general conditions.

In this paper, we present a discussion on the applicability of using separation of variables for a translating flexible beam. We present the notion of group velocity for dispersive waves and a nondimensionalized Euler–Bernoulli beam equation based on this group velocity. We show that if the beam is translating at a constant, slow (compared to the group velocity) speed, the assumed modes method can be used. The use of clamped-mass boundary conditions lead to a time-dependent frequency equation for the translating flexible beam. We present a novel method to solve this time-dependent frequency equation by using a differential form of the transcendental frequency equation. We then present a systematic modeling procedure for spatial multi-link flexible manipulator shaving both revolute and prismatic joints. The flexibility of links is approximated by using the assumed modes method. The Lagrangian formulation of dynamics is employed to derive closed form equations of motion. We show that the closed-loop dynamic response of modal variables become unstable during retraction of a flexible link, compared to the stable dynamic response during extension of the link by using a model-based control law. We present dynamic simulation results for a spatial RRP (Stanford Arm) configuration robot with prismatic jointed link modeled as a flexible link, and show that the results compare favorably with a finite element-based model.

II. MODELING OF A TRANSLATING FLEXIBLE BEAM

Fig. 1 shows a uniform flexible beam, of length $l(t)$, vibrating in the Z-X plane and moving axially at a velocity $U(t)$ along the Z direction. The portion of the beam to the left of origin of the fixed coordinate system is assumed not to be vibrating and any point along the neutral axis of the beam is located by s. We assume that the beam is inextensible along its neutral axis and hence the axial velocity is independent of s [13]. The free vibration equation of such a beam can be obtained by using the Euler–Bernoulli beam theory (neglecting the
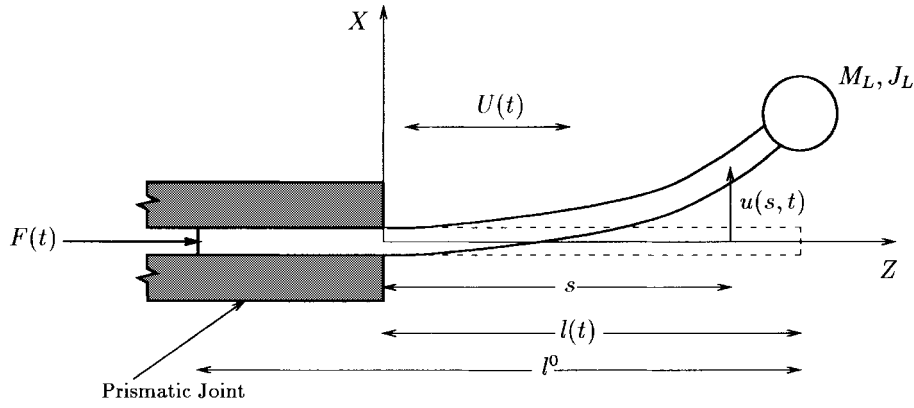
Fig. 1.   A schematic of the prismatic jointed flexible link with clamped and end-mass conditions.

shear deformation and rotary inertia effects), and is given by

$$EI\frac{\partial^4 u(s,t)}{\partial s^4} + \rho A\left(\frac{\partial^2 u(s,t)}{\partial t^2} + 2U\frac{\partial^2 u(s,t)}{\partial s \partial t}\right.$$
$$\left. +U^2\frac{\partial^2 u(s,t)}{\partial s^2} + \frac{dU}{dt}\frac{\partial u(s,t)}{\partial s}\right) = 0 \qquad (1)$$

where $s \in (0, l(t))$, $u(s,t)$ is the lateral deflection, EI is the flexural rigidity, ρ is the density of the material, and A is the cross-sectional area of the link. The boundary conditions for the above partial differential equation (1), for the clamped-mass case, are given as

$$[u(s,t)]_{s=0} = 0$$
$$EI\left[\frac{\partial^2 u(s,t)}{\partial s^2}\right]_{s=l(t)} = -J_L\left[\frac{\partial^3 u(s,t)}{\partial t^2 \partial s}\right]_{s=l(t)}$$
$$\left[\frac{\partial u(s,t)}{\partial s}\right]_{s=0} = 0$$
$$EI\left[\frac{\partial^3 u(s,t)}{\partial s^3}\right]_{s=l(t)} = M_L\left[\frac{\partial^2 u(s,t)}{\partial t^2}\right]_{s=l(t)} \qquad (2)$$

where M_L, J_L are the mass and rotary inertia of the load at end of the link (see Fig. 1).

Equation (1) contains the convective terms $2U(\partial^2 u(s,t)/\partial s \partial t)$, $U^2(\partial^2 u(s,t)/\partial s^2)$, and $(dU/dt)(\partial u(s,t)/\partial s)$, and if the axial velocity (U) is zero, it reduces to the standard Euler–Bernoulli beam equation with clamped-mass boundary conditions. The above equation also represents a moving boundary value problem as the domain governed by this equation changes with time. In this most general form, the above partial differential equation cannot be solved using the separation of variables method, as this method requires the general shape of the beam displacement not to change with time, while only the amplitude of this shape to change with time [20]. Therefore, it is required that the numerical solution to the partial differential equation (1) will have to be determined by using either finite difference or finite element-based schemes. It should be noted that these numerical schemes are however computationally very expensive for a specified numerical accuracy and special programming considerations are necessary. Moreover, as the finite element model uses polynomial mode shape functions which do not belong to the class of *complete* set of functions, monotonic convergence to actual solution cannot always be guaranteed [19]. However, convergence can be improved by considering large number of elements in the model. In the rest of the section, we present conditions under which the separation of variables and the assumed modes method can be used to solve the above problem.

Let us introduce the nondimensional variables: $\eta = s/l^0$, and $\tau = t/(l^0/U_g)$ with $U_g = (1/l^0)\sqrt{EI/\rho A}$. Note that η, τ, and U_g are based on the fully extended length of the beam l^0, as this would give the worst case. The quantity U_g is the "group velocity" of the dispersive waves of the Euler–Bernoulli beam equation [21] and l^0/U_g denotes the time taken for any disturbance to travel a distance of l^0. We observe that for a rigid body $(EI \to \infty)$, the time (l^0/U_g) taken for the disturbance to travel over the entire domain (l^0) approaches zero. On the other hand, for a highly flexible beam $(EI$ is small) or for a very long beam $(l^0$ is large), the time for the disturbance to travel the entire domain will be large. It may be mentioned that for times smaller than l^0/U_g the vibratory motion of the beam is *not* governed by (1) and the boundary conditions in (2). For times much greater than l^0/U_g however, one can assume a "quasi-steady" state, i.e., one can use the instantaneous mode shapes of the cantilever beam.

Rewriting the partial differential equation in terms of the nondimensional variables, η, τ and the ratio U/U_g, we get

$$\frac{\partial^4 u(\eta,\tau)}{\partial \eta^4} + \frac{\partial^2 u(\eta,\tau)}{\partial \tau^2} + 2\left(\frac{U}{U_g}\right)\frac{\partial^2 u(\eta,\tau)}{\partial \eta \partial \tau}$$
$$+ \left(\frac{U}{U_g}\right)^2\frac{\partial^2 u(\eta,\tau)}{\partial \eta^2} + \left(\frac{d}{d\tau}\left(\frac{U}{U_g}\right)\right)\frac{\partial u(\eta,\tau)}{\partial \eta} = 0$$
$$(3)$$

with the clamped-mass boundary conditions

$$[u(\eta,\tau)]_{\eta=0} = 0$$
$$\left[\frac{\partial^2 u(\eta,\tau)}{\partial \eta^2}\right]_{\eta=l(t)/l^0} = -\frac{J_L}{\rho A l^{03}}\left[\frac{\partial^3 u(\eta,\tau)}{\partial \tau^2 \partial \eta}\right]_{\eta=l(t)/l^0}$$
$$\left[\frac{\partial u(\eta,\tau)}{\partial \eta}\right]_{\eta=0} = 0$$
$$\left[\frac{\partial^3 u(\eta,\tau)}{\partial \eta^3}\right]_{\eta=l(t)/l^0} = \frac{M_L}{\rho A l^0}\left[\frac{\partial^2 u(\eta,\tau)}{\partial \tau^2}\right]_{\eta=l(t)/l^0}. \qquad (4)$$

We can make some observations from (3) and (4) (see below).

1) The coefficients of the first two terms are unity and the third, fourth and fifth terms are in terms of U/U_g and the derivative of U/U_g with respect to τ. For a constant axial velocity, the term containing the derivative of U/U_g with respect to τ is zero. For the third and fourth terms to be dominant U/U_g should be large.

2) The ratio U/U_g, for a given U, is largest for the smallest U_g. The smallest U_g is obtained when the beam is fully extended, i.e., when $l = l^0$.

3) If $U/U_g \ll 1$, then by dimensional analysis we can drop the third and fourth terms. In typical simulations and experiments

[11], U is approximately 0.1 m/s, and U_g is approximately 3.03 m/s giving $U/U_g \approx 0.033 \ll 1$. Hence the convective terms can be easily neglected. We have run simulations with various axial speeds U, up to 1 m/s with $U_g = 59.34$ m/s, and have observed that the contribution of the convective terms are much smaller compared to the first two terms. In particular, the tip deflections obtained after neglecting the convective terms match quite accurately with those obtained from a FEM-based model derived from the complete partial differential equation [19]. In this paper, we present numerical simulations, with $U \approx 0.778$ m/s and smallest $U_g = 59.34$ m/s

4) Once the convective terms are dropped, we are left with the standard Euler–Bernoulli beam equation for a clamped-mass cantilever. Separation of variables or the assumed modes method can then be used with the eigen-frequencies based on the fully extended length l_0. Even if the lengthis changing continuously with time (slowly compared to U_g) we can still assume that the "eigen-modes" can be used, i.e., the mode shape of the translating beam at every instant of time can be approximated by that of a cantilever beam [11]. However, we have to solve for the slowly and continuously changing "eigen-frequencies" (often called "quasi-frequencies" [18]) at each instant of time. This procedure is illustrated below.

Let the lateral deflection be described as $u(\eta, \tau) = \boldsymbol{\psi}(\eta)^T \boldsymbol{\xi}(\tau)$, where spatial admissible functions $\boldsymbol{\psi}(\eta) \equiv [\psi_1(\eta), \psi_2(\eta), \cdots, \psi_n(\eta)]^T$ are the *complete* eigen functions (in the sense that for arbitrary square-integrable $u(\eta, \tau)$: $\min \| u(\eta, \tau) - \boldsymbol{\psi}(\eta)^T \boldsymbol{\xi}(\tau)\|^2 = 0$). Then, following the standard procedure of assumed modes method, we can write

$$\frac{d^4\psi_i(\eta)}{d\eta^4}\xi_i(\tau) + \psi_i(\eta)\frac{d^2\xi_i(\tau)}{d\tau^2} = 0 \qquad i = 1, 2, \cdots, n. \quad (5)$$

For separation of variables, the ratio $(d^2\xi_i(\tau)/d\tau^2)/\xi_i(\tau) = -(d^4\psi_i(\eta)/d\eta^4)/\psi_i(\eta)$ must be constant. This constant is usually denoted by $-\omega_i^2$ and are called the "eigen-frequencies" of the system (5). These eigen-frequencies are related to the roots (β_i) of the frequency equation (also called the "wave number" of system (5)) by the dispersion relation [21], $\omega_i = U_g/l\beta_i^2$. It can be seen that when length of the vibrating beam (l) changes continuously with time, these eigen-frequencies will also change continuously with time irrespective of β_i which are determined by the end-conditions.

5) We observe from the boundary conditions (4) that it is reasonable to use "free" end-conditions for the choice of eigen functions $(\psi_i(\eta))$ only if $J_L/\rho Al^3 \ll 1$ and $M_L/\rho Al \ll 1$, when the beam is fully extended (i.e., $l = l^0$). On the other hand, if the rotary inertia (J_L) and mass (M_L) of the load are comparable to that of the vibrating beam, it is more appropriate and correct to use the "mass" end-conditions. However, this mass end-conditions lead to time-dependent frequency equations as shown below.

The eigen functions $\psi(\eta)$ satisfying the "clamped-mass" boundary conditions are given by

$$\psi_i(\eta) = C_i[\cos(\beta_i\eta) - \cosh(\beta_i\eta) + \nu_i(\sin(\beta_i\eta) - \sinh(\beta_i\eta))] \quad (6)$$

where

$$\nu_i = \frac{\sin\beta_i - \sinh\beta_i + M\beta_i(\cos\beta_i - \cosh\beta_i)}{\cos\beta_i + \cosh\beta_i - M\beta_i(\sin\beta_i - \sinh\beta_i)} \quad (7)$$

and β_i are solutions of the frequency equation

$$(1 + \cosh\beta_i\cos\beta_i) - M\beta_i(\cosh\beta_i\sin\beta_i - \sinh\beta_i\cos\beta_i)$$
$$- J\beta_i^3(\cosh\beta_i\sin\beta_i + \sinh\beta_i\cos\beta_i)$$
$$+ MJ\beta_i^4(1 - \cosh\beta_i\cos\beta_i) = 0 \quad (8)$$

where $M = M_L/\rho Al, J = J_L/\rho Al^3$. The C_i are constants which normalizes the eigen functions. It can be seen from (8) that when "clamped-free" end-conditions are used the roots (β_i) of the equation will be constants, however with the "clamped-mass" end-conditions they will change with time, albeit slowly. The slowly changing nature of β_i is shown in our numerical simulations (see Section V).

6) The time-dependent frequency equation can be solved by either using a root finding algorithm at each instant of time or by using a "table look-up" approach [22]. The former approach may lead to considerable increase in computational time, while the latter requires a large storage space for the specified accuracy. In the following, we present a novel method to solve time-dependent frequency equation using differential form of the equation, which then can be solved together with the dynamic equations of motion.

Let us rewrite the clamped-mass frequency equation (8) as

$$f(\beta_i, l) = (1 + \cosh\beta_i\cos\beta_i) - \frac{M_L\beta_i}{\rho Al}$$
$$\cdot(\cosh\beta_i\sin\beta_i - \sinh\beta_i\cos\beta_i)$$
$$- \frac{J_L\beta_i^3}{\rho Al^3}(\cosh\beta_i\sin\beta_i + \sinh\beta_i\cos\beta_i)$$
$$+ \frac{M_L J_L\beta_i^4}{\rho^2 A^2 l^4}(1 - \cosh\beta_i\cos\beta_i) = 0. \quad (9)$$

Since the frequency equation is continuous in β_i and the roots of the frequency equation are all distinct, we can differentiate (9) with respect to time

$$\frac{df(\beta_i, l)}{dt} = \frac{\partial f(\beta_i, l)}{\partial \beta_i}\frac{d\beta_i}{dt} + \frac{\partial f(\beta_i, l)}{\partial l}\frac{dl}{dt} = 0 \quad (10)$$

and rearrange to obtain

$$\frac{d\beta_i}{dt} = \frac{f_1(\beta_i, l)}{f_2(\beta_i, l)}\frac{dl}{dt} \quad (11)$$

where

$$f_1(\beta_i, l) = \frac{M_L}{\rho Al^2}\beta_i(\sinh\beta_i\cos\beta_i - \cosh\beta_i\sin\beta_i)$$
$$- \frac{3J_L}{\rho Al^4}\beta_i^3(\sinh\beta_i\cos\beta_i + \cosh\beta_i\sin\beta_i)$$
$$+ \frac{4M_L J_L}{\rho^2 A^2 l^5}\beta_i^4(1 - \cosh\beta_i\cos\beta_i) \quad (12)$$

and

$$f_2(\beta_i, l) = \left[1 + \frac{M_L}{\rho Al}\left(1 - \frac{J_L}{\rho Al^3}\beta_i^4\right)\right]$$
$$\cdot(\sinh\beta_i\cos\beta_i - \cosh\beta_i\sin\beta_i)$$
$$- \frac{3J_L}{\rho Al^3}\beta_i^2(\sinh\beta_i\cos\beta_i + \cosh\beta_i\sin\beta_i)$$
$$+ \frac{2J_L}{\rho Al^3}\beta_i^3\left[\frac{2M_L}{\rho Al} - \left(1 + \frac{2M_L}{\rho Al}\right)\cosh\beta_i\cos\beta_i\right]$$
$$- \frac{2M_L}{\rho Al}\beta_i\sinh\beta_i\sin\beta_i. \quad (13)$$

This ordinary differential equation (11) on β_i, which is now a function of the generalized variables $(l$ and $dl/dt)$, can then be solved together with the dynamic equations of motion of the system, with the initial
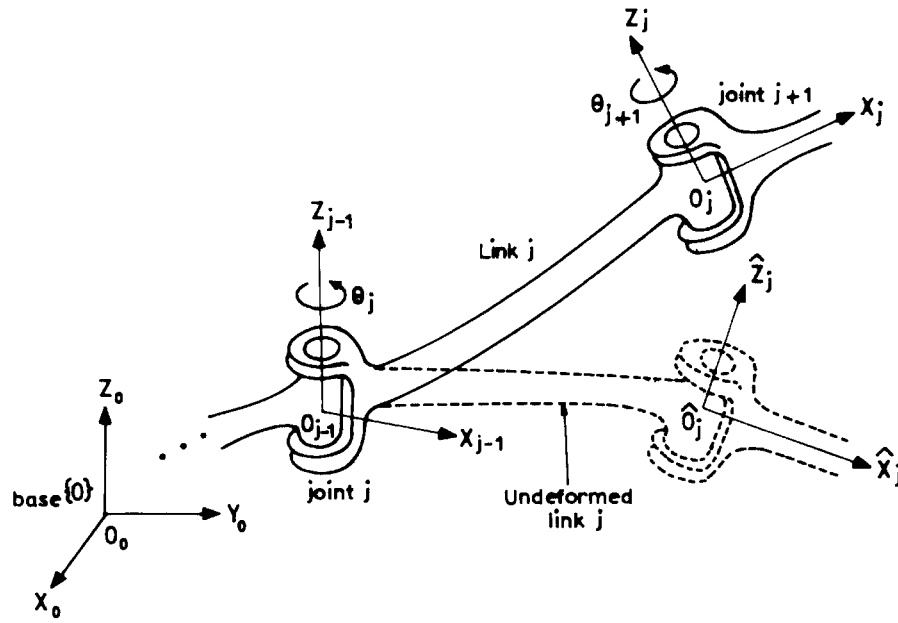
Fig. 2. Coordinate systems for the flexible link j.

condition $\beta_i(t = 0)$ solved from the frequency equation (9) for $l(t = 0)$.

In summary, we can conclude that although the eigenfunctions $\psi_i(\eta)$ [see (6)] does not strictly satisfy the partial differential equation (3), the translating flexible beam can be quite accurately modeled as an instantaneous clamped-mass cantilever beam if the axial velocity U is constant and small compared to the group velocity U_g. We can assume that the separation of variables method can still be used, however, we need to take into account the slowly changing "eigen-frequencies". The time-dependent frequency equation due to the clamped-mass boundary conditions can be solved using a differential form of the equation together with the equations of motion.

III. MODELING OF FLEXIBLE-LINK MANIPULATORS

The dynamics of rigid-arm manipulators is characterized by a system of nonlinear, coupled, ordinary differential equations [23], but manipulators with flexible links being continuous (distributed) dynamical systems, are governed by nonlinear, coupled, ordinary, and partial differential equations [1]. In this section, we use the assumed modes model to approximate the flexibility of links (see previous section). We consider only the bending vibrations of flexible links[1]. The link deflections with reference to its rigid configuration are, however, assumed to be small.

A. Flexible-Arm Kinematics

By convention, the links of a flexible manipulator are numbered consecutively from 0 to n starting from base of the manipulator to tip of the end-effector, where n is the total number of links. We define the coordinate system (X_j, Y_j, Z_j) on link j with origin O_j at the distal end (farthest from the base), oriented so that the Z_j axis is along the axis of joint $j + 1$. We also define the coordinate system $(\hat{X}_j, \hat{Y}_j, \hat{Z}_j)$ on link j with origin $\hat{O}_j$ in such a way that when the link is in its undeformed configuration, the coordinate system (X_j, Y_j, Z_j) is exactly coincident on the coordinate system $(\hat{X}_j, \hat{Y}_j, \hat{Z}_j)$ (see Fig. 2).

[1] For most robotic manipulators in general, we can neglect the axial and torsional vibration components of the links because of their much greater rigidity in the axial direction and due to the structural design of robotic systems.
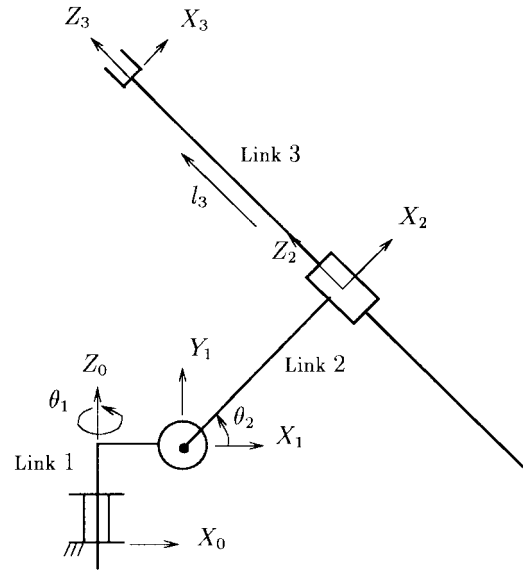

Fig. 3. Flexible spherical (RRP) manipulator.

The 4×4 homogeneous transformation matrix from coordinate system $(\hat{X}_j, \hat{Y}_j, \hat{Z}_j)$ to coordinate system $(X_{j-1}, Y_{j-1}, Z_{j-1})$ is given by

$$
A_j^{j-1}
$$
$$
= \begin{pmatrix}
\cos\theta_j & -\sin\theta_j \cos\alpha_j & \sin\theta_j \sin\alpha_j & a_j \cos\theta_j \\
\sin\theta_j & \cos\theta_j \cos\alpha_j & -\cos\theta_j \sin\alpha_j & a_j \sin\theta_j \\
0 & \sin\alpha_j & \cos\alpha_j & d_j \\
0 & 0 & 0 & 1
\end{pmatrix}
$$
(14)

where θ_j, α_j, d_j, and a_j are the Denavit–Hartenberg parameters [23] representing relationship between coordinate systems $(\hat{X}_j, \hat{Y}_j, \hat{Z}_j)$ and $(X_{j-1}, Y_{j-1}, Z_{j-1})$. Throughout this paper, $q_{r_j}(t)$ denotes the joint variable: it is θ_j if joint j is revolute, and d_j if the joint is prismatic. Note that for the link with prismatic joint, $a_j = 0$. The 4×4 homogeneous transformation matrix from coordinate system

(X_j, Y_j, Z_j) to $(\hat{X}_j, \hat{Y}_j, \hat{Z}_j)$, caused by the deformation of link j—assuming small elasticde formations [1] is given by

$$E_j^{j-1} = \begin{pmatrix} 1 & -\phi_{z_j} & \phi_{y_j} & \delta_{x_j} \\ \phi_{z_j} & 1 & -\phi_{x_j} & \delta_{y_j} \\ -\phi_{y_j} & \phi_{x_j} & 1 & \delta_{z_j} \\ 0 & 0 & 0 & 1 \end{pmatrix} \tag{15}$$

where $\phi_j = (\phi_{x_j}, \phi_{y_j}, \phi_{z_j})^T$ and $\delta_j = (\delta_{x_j}, \delta_{y_j}, \delta_{z_j})^T$ describe the rotation and translation between the coordinate systems $(\hat{X}_j, \hat{Y}_j, \hat{Z}_j)$ and (X_j, Y_j, Z_j), respectively. Let $\hat{T}_j^0$ and T_j^0 be the 4×4 homogeneous transformation matrices from coordinate systems $(\hat{X}_j, \hat{Y}_j, \hat{Z}_j)$ and (X_j, Y_j, Z_j) to the base coordinate system (X_0, Y_0, Z_0), respectively, then

$$\hat{T}_j^0 = \begin{pmatrix} \hat{R}_j^0 & \hat{p}_j^0 \\ 0 & 1 \end{pmatrix} = A_1^0 E_1^0 \cdots A_{j-1}^{j-2} E_{j-1}^{j-2} A_j^{j-1} \tag{16}$$

and

$$T_j^0 = \begin{pmatrix} R_j^0 & p_j^0 \\ 0 & 1 \end{pmatrix} = A_1^0 E_1^0 \cdots A_{j-1}^{j-2} E_{j-1}^{j-2} A_j^{j-1} E_j^{j-1} \tag{17}$$

where $\hat{R}_j^0 (R_j^0)$ is the 3×3 rotation matrix, $\hat{p}_j^0 (p_j^0)$ is the 3×1 position vector, and 0 is the 1×3 zero vector.

Using this notation, the position vector of any point (s) along the neutral axis of link j can be expressed with reference to the base coordinate system (X_0, Y_0, Z_0) as

$$r_j^0 = p_{j-1}^0 + \hat{R}_j^0 r_j \tag{18}$$

where

$$r_j = \begin{cases} \begin{pmatrix} s \\ 0 \\ 0 \end{pmatrix} + \begin{pmatrix} 0 \\ v_j(s,t) \\ w_j(s,t) \end{pmatrix} & \text{if joint } j \text{ is revolute} \\ \begin{pmatrix} 0 \\ 0 \\ s \end{pmatrix} + \begin{pmatrix} u_j(s,t) \\ v_j(s,t) \\ 0 \end{pmatrix} & \text{if joint } j \text{ is prismatic} \end{cases} \tag{19}$$

and $u_j(s,t), v_j(s,t), w_j(s,t)$ are displacements with reference to the neutral axis of flexible link j at a distance s and at time t, due to flexibility in the respective directions. Note that the dependence of u_j, v_j, w_j on the spatial coordinate (s), makes the system infinite dimensional, leading to coupled ordinary and partial differential equations of motion.

The velocity of the point (s) on link j can be obtained from the time derivative of the position vector in the inertial base frame $\{0\}$, and is given by

$$\dot{r}_j^0 = \dot{p}_{j-1}^0 + \dot{\hat{R}}_j^0 r_j + \hat{R}_j^0 \dot{r}_j \tag{20}$$

where an overdot indicates the time derivative operator.

Assuming that the flexible displacements, $u_j(s,t), v_j(s,t), w_j(s,t)$ can be discretized by assumed modes method (see Section II), we can write

$$u_j(\eta, t) = \sum_{i=1}^{n_j} \psi_i^{u_j}(\eta) \xi_i^{u_j}(t)$$

$$v_j(\eta, t) = \sum_{i=1}^{n_j} \psi_i^{v_j}(\eta) \xi_i^{v_j}(t)$$

$$w_j(\eta, t) = \sum_{i=1}^{n_j} \psi_i^{w_j}(\eta) \xi_i^{w_j}(t) \tag{21}$$

where $\eta = s/l_j, l_j$ is the length of flexible link j, and n_j is the number of modes used to describe the deflection of link j. It should be noted that when we consider the flexible link with a revolute joint, the length of the vibrating link $l_j \equiv a_j$, remains constant. On the other hand, if for a flexible link with a prismatic joint, the length of the vibrating link $l_j \equiv d_j$ would vary with time (t) as the length d_j of the translating beam is the joint variable.

We choose "clamped-mass" eigen functions for flexible links of the manipulator system. The clamped-mass end-conditions lead to time-dependent frequency equation as shown in Section II, for the translating flexible link, and for revolute jointed flexible-link manipulators with more than onelink [4], [19].

The 4×4 homogeneous transformation matrix, E_j^{j-1} that describes the link deformations for link j, can now be written as

if joint j is revolute, (see (22) at the bottom of the page)

if joint j is prismatic, (see (23) at the bottom of the page) where I is the 4×4 identity matrix and note that all variables in the transformation matrix are evaluated at $\eta = 1$, tip of the link j. The generalized flexible deformation variables in this case are therefore, $q_{f_j} = (\xi_1^{u_j}(t), \xi_1^{v_j}(t), \xi_1^{w_j}(t), \cdots, \xi_{n_j}^{u_j}(t), \xi_{n_j}^{v_j}(t), \xi_{n_j}^{w_j}(t))^T$. The velocity of any point on flexible link j expressed in undeformed local link coordinate system is given by (see (24) at the bottom of the next page).

$$E_j^{j-1} = I + \sum_{i=1}^{n_j} \begin{pmatrix} 0 & -\dfrac{\partial \psi_i^{v_j}(1)}{\partial \eta} \xi_i^{v_j}(t) & \dfrac{\partial \psi_i^{w_j}(1)}{\partial \eta} \xi_i^{w_j}(t) & 0 \\ \dfrac{\partial \psi_i^{v_j}(1)}{\partial \eta} \xi_i^{v_j}(t) & 0 & 0 & \psi_i^{v_j}(1) \xi_i^{v_j}(t) \\ -\dfrac{\partial \psi_i^{w_j}(1)}{\partial \eta} \xi_i^{w_j}(t) & 0 & 0 & \psi_i^{w_j}(1) \xi_i^{w_j}(t) \\ 0 & 0 & 0 & 0 \end{pmatrix} \tag{22}$$

$$E_j^{j-1} = I + \sum_{i=1}^{n_j} \begin{pmatrix} 0 & 0 & \dfrac{\partial \psi_i^{u_j}(1)}{\partial \eta} \xi_i^{u_j}(t) & \psi_i^{u_j}(1) \xi_i^{u_j}(t) \\ 0 & 0 & -\dfrac{\partial \psi_i^{v_j}(1)}{\partial \eta} \xi_i^{v_j}(t) & \psi_i^{v_j}(1) \xi_i^{v_j}(t) \\ -\dfrac{\partial \psi_i^{u_j}(1)}{\partial \eta} \xi_i^{u_j}(t) & \dfrac{\partial \psi_i^{v_j}(1)}{\partial \eta} \xi_i^{v_j}(t) & 0 & 0 \\ 0 & 0 & 0 & 0 \end{pmatrix} \tag{23}$$

B. Dynamic Equations of Motion

The dynamic equations of motion are obtained using the Lagrange's formulation of dynamics. It may be noted that the generalized force corresponding to joint variable q_{r_j} is the joint input Γ_j (torque τ_j for a revolute joint, or force F_j for a prismatic joint). For the flexible deformation variables (q_f) the corresponding generalized force will be "zero", if the corresponding elastic deflections or rotations have no displacement at those locations where external forces are applied, and note that this corresponds to the case when "clamped" condition is used for controlled end of the link [1]. It should be noted that other conditions for controlled end of the link, such as "pinned" condition, or "free" condition will have "nonzero" generalized forces corresponding to the generalized flexible deformation variables.

The general form of Lagrange's equations (for clamped condition) are then, for joint variable q_{r_j}

$$\frac{d}{dt}\left(\frac{\partial T}{\partial \dot{q}_{r_j}}\right) - \frac{\partial T}{\partial q_{r_j}} + \frac{\partial V}{\partial q_{r_j}} = \Gamma_j \tag{25}$$

for flexible deformation variable $q_{f_{ji}}$

$$\frac{d}{dt}\left(\frac{\partial T}{\partial \dot{q}_{f_{ji}}}\right) - \frac{\partial T}{\partial q_{f_{ji}}} + \frac{\partial V}{\partial q_{f_{ji}}} = 0 \tag{26}$$

where T is the total kinetic energy of the flexible manipulator system, and V is the total potential energy due to elastic deformations and gravity.

1) Kinetic Energy: The total kinetic energy of flexible-link manipulator system is due to the motions of joints and links, and kinetic energy due to the payload. The kinetic energy for a revolute joint j, if considered as mass with rotary inertia about the axis of revolution is given by

$$T_{\text{joint}_j} = \frac{1}{2}\Omega_j^{0^T} \boldsymbol{I}_j \Omega_j^0 + \frac{1}{2}m_j\left(\frac{d\boldsymbol{p}_{j-1}^0}{dt}\right)^T \left(\frac{d\boldsymbol{p}_{j-1}^0}{dt}\right) \tag{27}$$

where m_j is the mass of the joint hub j, $\boldsymbol{p}_{j-1}^0$ is position vector of the joint j, $\boldsymbol{I}_j$, and Ω_j^0 are the joint inertia matrix, and the angular velocity vector of joint j, respectively. In the case of prismatic joint j, at any instant of time, a part of the translating beam is outside the joint hub and is free to vibrate, while the remaining part of the beam is inside the joint hub and is restrained from vibrating [11]. The kinetic energy due to part of the beam inside the joint hub is given by

$$T_{\text{joint}_j} = \frac{1}{2}\int_{(l_j(t)-l_j^0)}^0 \rho_j A_j \left(\frac{d\hat{\boldsymbol{r}}_j^0}{dt}\right)^T \left(\frac{d\hat{\boldsymbol{r}}_j^0}{dt}\right) ds \tag{28}$$

where

$$\hat{\boldsymbol{r}}_j^0 = \boldsymbol{p}_{j-1}^0 + s\hat{\boldsymbol{z}}_j^0$$

and $\hat{\boldsymbol{z}}_j^0$ is the third column vector of the rotation matrix $\hat{\boldsymbol{R}}_j^0$, and $l_j^0, l_j(t)$ are the total length of the translating beam, and length of the beam outside the joint hub at time t, respectively.

Under the assumption that the links are slender beams [20], the kinetic energy of the flexible link j can be obtained as

$$T_{\text{link}_j} = \frac{1}{2}\int_0^{l_j} \rho_j A_j \left(\frac{d\boldsymbol{r}_j^0}{dt}\right)^T \left(\frac{d\boldsymbol{r}_j^0}{dt}\right) ds \tag{29}$$

where ρ_j is the density of the material, A_j is the cross-sectional area, and l_j is the length of flexible link j.

The kinetic energy due to the payload is given by

$$T_{\text{payload}} = \frac{1}{2}m_p\left(\frac{d\boldsymbol{p}_n^0}{dt}\right)^T \left(\frac{d\boldsymbol{p}_n^0}{dt}\right) \tag{30}$$

where $\boldsymbol{p}_n^0$ is position vector of tip of the end-effector [see (17)], and m_p is mass of the payload.

2) Potential Energy The potential energy of the flexible manipulator system arises from two sources—due to the deformation of links and due to gravity. Assuming slender beam type of links and neglecting the axial and torsional vibration of links, the potential energy due to bending deformations of link j about the transverse $\hat{Y}_j$ and $\hat{Z}_j$ axes, is given by [20]

$$V_{fj} = \frac{1}{2}\int_0^{l_j} \left(E_j I_{jy}\left(\frac{\partial^2 v_j(s,t)}{\partial s^2}\right)^2 + E_j I_{jz}\left(\frac{\partial^2 w_j(s,t)}{\partial s^2}\right)^2\right) ds \tag{31}$$

where E_j is the Young's modulus, I_{jy}, I_{jz} are the area moments of inertia about respective axes, of link j. Note that for flexible link j with prismatic joint, the bending deformations of the link in the transverse $\hat{X}_j$ and $\hat{Y}_j$ axes have to be considered as opposed to the above equation.

The gravitational potential energy due to the mass of joint hub and due to the elastic link j is of the form

$$V_{gj} = m_j \boldsymbol{g}^T \boldsymbol{p}_{j-1}^0 + \int_0^{l_j} \rho_j A_j \boldsymbol{g}^T \boldsymbol{r}_j^0 \, ds \tag{32}$$

where $\boldsymbol{g}$ is the gravity vector in the inertial coordinate system $\{0\}$. The gravitational potential energy due to the payload mass is given by

$$V_{g_{\text{payload}}} = m_p \boldsymbol{g}^T \boldsymbol{p}_n^0. \tag{33}$$

The system's total potential energy (V) is then, sum of potential energies [(31) and (32)] over all the links, and due to the payload (33).

The closed form dynamic equations of motion for flexible-link manipulators can be derived using symbolic manipulation software

$$\dot{\boldsymbol{r}}_j = \begin{cases} \begin{pmatrix} 0 \\ \sum_{i=1}^{n_j}\psi_i^{v_j}(\eta)\dfrac{d\xi_i^{v_j}(t)}{dt} \\ \sum_{i=1}^{n_j}\psi_i^{w_j}(\eta)\dfrac{d\xi_i^{w_j}(t)}{dt} \end{pmatrix} & \text{if joint } j \text{ is revolute} \\[4ex] \begin{pmatrix} \sum_{i=1}^{n_j}\left[\psi_i^{u_j}(\eta)\dfrac{d\xi_i^{u_j}(t)}{dt} - \dfrac{\partial\psi_i^{u_j}(\eta)}{\partial\eta}\dfrac{\xi_i^{u_j}(t)\eta}{l_j(t)}\dfrac{dl_j(t)}{dt}\right] \\ \sum_{i=1}^{n_j}\left[\psi_i^{v_j}(\eta)\dfrac{d\xi_i^{v_j}(t)}{dt} - \dfrac{\partial\psi_i^{v_j}(\eta)}{\partial\eta}\dfrac{\xi_i^{v_j}(t)\eta}{l_j(t)}\dfrac{dl_j(t)}{dt}\right] \\ \dfrac{dl_j(t)}{dt} \end{pmatrix} & \text{if joint } j \text{ is prismatic} \end{cases} \tag{24}$$
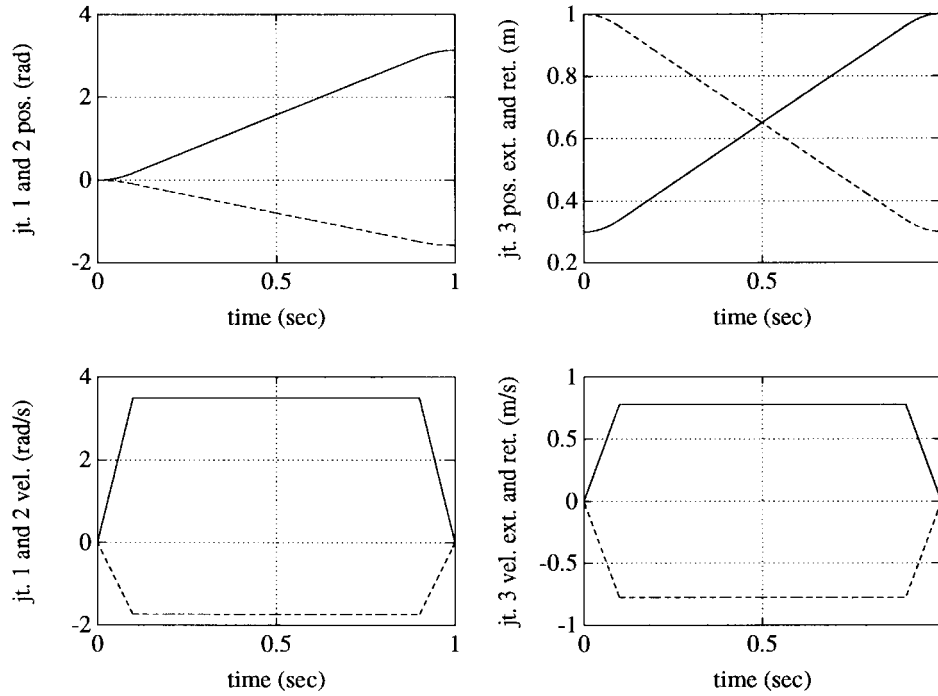
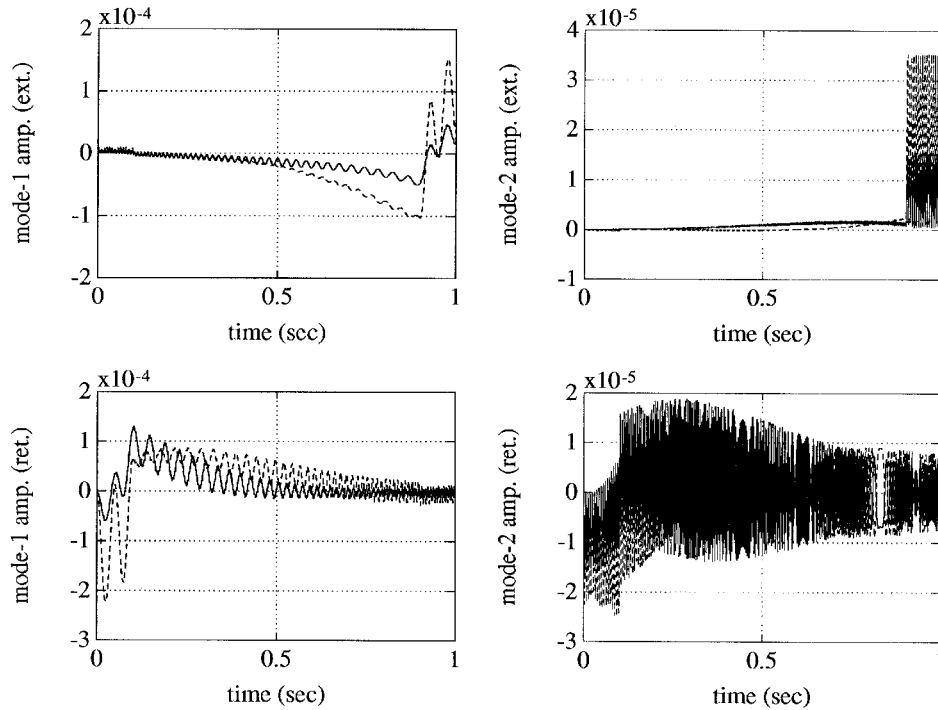Fig. 4.   Desired joint positions and velocities.

Fig. 5.   Time history of the vibration mode amplitudes during extension and retraction of the link 3 (——: in-plane vibration, - - -: out-of-plane vibration).

such as REDUCE or MACSYMA. The resulting equations of motion in the matrix form can be written as

$$\begin{pmatrix} M_{rr} & M_{rf} \\ M_{rf}^T & M_{ff} \end{pmatrix} \begin{pmatrix} \ddot{q}_r \\ \ddot{q}_f \end{pmatrix} + \begin{pmatrix} h_r(q,\dot{q}) \\ h_f(q,\dot{q}) \end{pmatrix} + \begin{pmatrix} c_r(q) \\ c_f(q) \end{pmatrix}$$
$$+ \begin{pmatrix} 0 & 0 \\ 0 & K \end{pmatrix} \begin{pmatrix} q_r \\ q_f \end{pmatrix} = \begin{pmatrix} \Gamma \\ 0 \end{pmatrix} \qquad (34)$$

where $q = (q_r^T, q_f^T)^T$, is the n-vector of generalized joint (q_r),

and N-vector of flexible deformation (q_f) variables, M is the $(n+N) \times (n+N)$ configuration dependent generalized mass matrix, h is the $(n+N)$-vector of Coriolis, and centrifugal terms and the terms accounting for the interaction of joint variables and their rates with flexible variables and their rates, c is the $(n+N)$-vector of gravitational terms, K is the $N \times N$ flexural structure stiffness matrix of the system, Γ is the n-vector of input torques (or forces) applied at the joints, and 0 is the zero matrix/vector with appropriate dimensions.
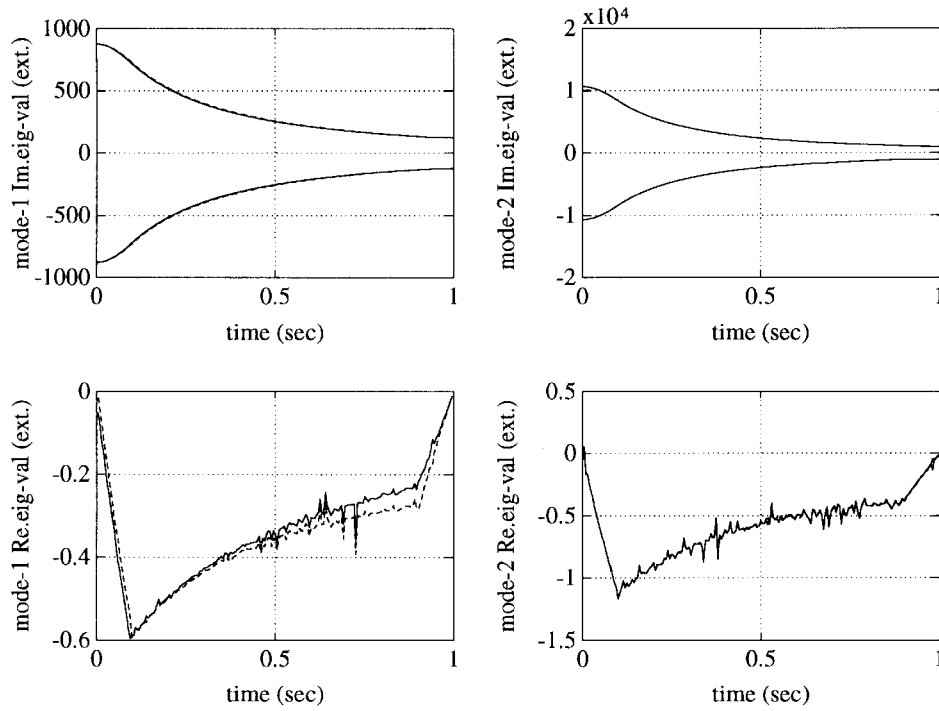
Fig. 6.   Time history of the closed-loop eigenvalues of flexible variables during extension of link 3 (——: in-plane vibration, - - -: out-of-plane vibration).
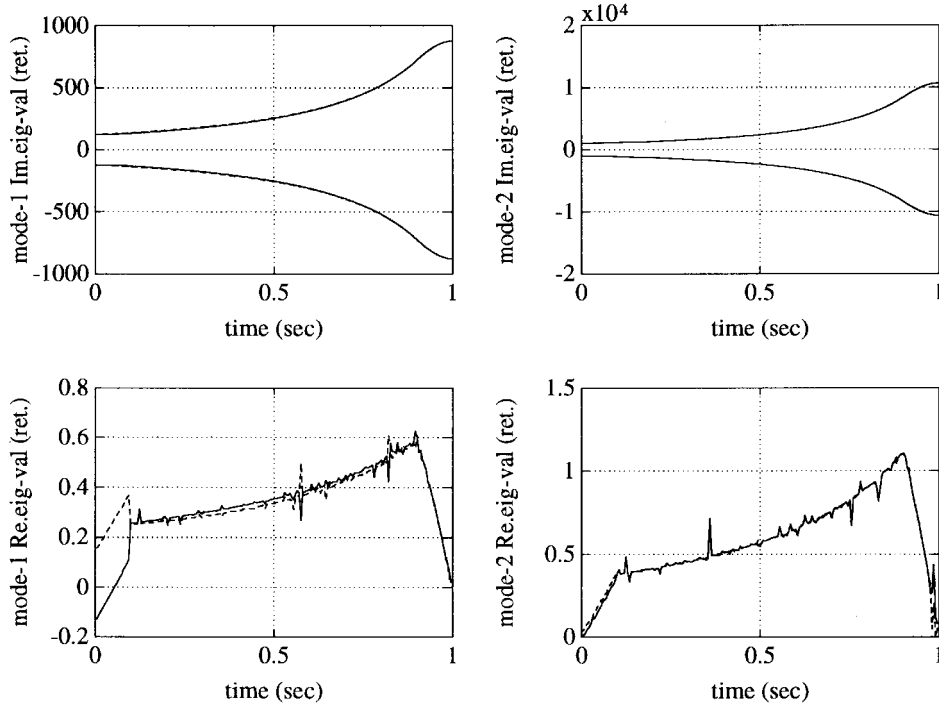

Fig. 7.   Time history of the closed-loop eigenvalues of flexible variables during retraction of link 3 (——: in-plane vibration, - - -: out-of-plane vibration).

IV. STABILITY ANALYSIS

In this section, we discuss the stability properties of manipulators with a prismatic jointed flexible link. We assume without loss of generality that the manipulator operates in a gravity-free environment (i.e., $c(q) \equiv 0$ in (34)). Let us suppose that the control input vector is calculated using the nonlinear decoupling technique applied to joints [3], [24], and is given by

$$\boldsymbol{\Gamma} = (\boldsymbol{M}_{rr} - \boldsymbol{M}_{rf}\boldsymbol{M}_{ff}^{-1}\boldsymbol{M}_{rf}^{T})\boldsymbol{u} + (\boldsymbol{h}_r - \boldsymbol{M}_{rf}\boldsymbol{M}_{ff}^{-1}(\boldsymbol{h}_f + \boldsymbol{K}\boldsymbol{q}_f)). \tag{35}$$

The new control input $\boldsymbol{u}$ can be chosen for a specified joint trajectory as

$$\boldsymbol{u} = \ddot{\boldsymbol{q}}_r^d(t) - \boldsymbol{G}_v\dot{\boldsymbol{e}}(t) - \boldsymbol{G}_p\boldsymbol{e}(t) \tag{36}$$

so that the joint error satisfies

$$\ddot{\boldsymbol{e}}(t) + \boldsymbol{G}_v\dot{\boldsymbol{e}}(t) + \boldsymbol{G}_p\boldsymbol{e}(t) = \boldsymbol{0} \tag{37}$$

where $\boldsymbol{e}(t) = \boldsymbol{q}_r(t) - \boldsymbol{q}_r^d(t)$, is the vector of joint errors, $\boldsymbol{G}_p$ and $\boldsymbol{G}_v$ are positive constant diagonal position and velocity gain matrices for the joint variables, respectively. The model-based controller [(35)
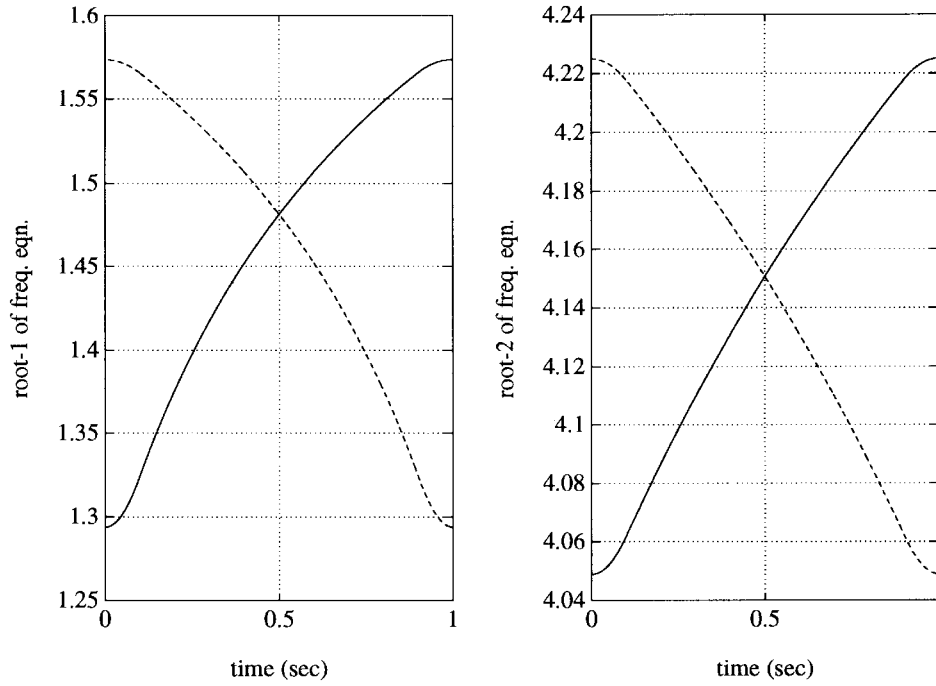
Fig. 8.   Time history of the solutions (β_i) of clamped-mass transcendental equation. (——: extension of link 3, - - -: retraction of link 3)

TABLE I
RRP CONFIGURATION ROBOT SYSTEM PARAMETERS

Physical system parameters	Value
mass of link 1 (m_1)	$3.7051 kg$
mass of link 2 (m_2)	$0.3310 kg$
mass of link 3 (m_3)	$0.4303 kg$
mass of payload (m_p)	$0.0828 kg$
length of link 1 (l_1)	$0.1 m$
length of link 2 (l_2)	$0.3 m$
total length of link 3 (l_3^0)	$1.3 m$
rotary inertia of joint 1 (I_1)	$0.352 kgm^2$
rotary inertia of joint 2 (I_2)	$3.2 kgm^2$
flexural rigidity of link 3 ($E_3 I_3$)	$1165.4916 Nm^2$

and (36)], thus results in the following set of closed-loop system of equations [19], [24]

$$\ddot{q}_r(t) = u \qquad (38)$$

$$M_{ff}\ddot{q}_f + h_f(q, \dot{q}) + K q_f = -M_{rf}^T u. \qquad (39)$$

We observe from the closed-loop system of (38) and (39) that a twice differentiable desired joint trajectory $q_r^d(t)$ will be asymptotically tracked for the proper choices of gain matrices G_p and G_v. However, the feasibility of this control law is based on the stability of (39) [24]. Let us consider "uniform motion" of the joint variables (i.e., $\ddot{q}_r^d(t) = 0$) with $e, \dot{e}$ equal to zero at $t = 0$. This results in the new control input $u = 0$, and we have

$$\ddot{q}_f = -M_{ff}^{-1}(h_f(q, \dot{q}) + K q_f) \qquad (40)$$

where a factorization of the type $h_f(q, \dot{q}) = N_{ff}(q, \dot{q})\dot{q}_f$ exists, with $\dot{M}_{ff} - 2N_{ff}$ skew-symmetric [24]. Let us then consider the following candidate Lyapunov function

$$V(t) = \frac{1}{2}(\dot{q}_f^T M_{ff} \dot{q}_f + q_f^T K q_f) \qquad (41)$$

vanishing only at the desired equilibrium state $(q_f^e, \dot{q}_f^e) = (0, 0)$ of system (40). The time derivative of the Lyapunov function (41) along the trajectories of system (40) is given by

$$\dot{V}(t) = \frac{1}{2}q_f^T \dot{K} q_f \qquad (42)$$

where

$$\dot{K} = \text{Diag}\left\{ -\frac{EI}{l^4(t)}\frac{dl(t)}{dt}\left[3\int_0^1 \left(\frac{d^2\psi_i}{d\eta^2}\right)^2 d\eta \right. \right.$$
$$\left. \left. + 2\int_0^1 \eta\left(\frac{d^2\psi_i}{d\eta^2}\right)\left(\frac{d^3\psi_i}{d\eta^3}\right)d\eta \right] \right\}. \qquad (43)$$

It may be seen in (43) above that the flexural rigidity, EI, and the length of the translating flexible beam, $l(t)$, are always positive. The terms inside the bracket are also positive. Hence the sign of $\dot{K}$ and $\dot{V}(t)$ are determined by the sign of $dl(t)/dt$. For extension of the link $dl(t)/dt > 0$ which implies $\dot{K} < 0$ and therefore $\dot{V}(t) < 0$ for all values of time (t). This implies that the dynamic response of the flexible modal variables (q_f) is stable during extension of the flexible link. For retraction of the link, $dl(t)/dt < 0$, which implies $\dot{K} > 0$ and therefore $\dot{V}(t) > 0$ and this may lead to unstable dynamic response of the flexible modal variables.

It should be mentioned that during extension of the flexible link, the amplitude of modal variables (A) increases as the frequency of vibration (ω_i) decreases so as to conserve the elastic energy (proportional to $A\omega_i^2$). However the motion is stable, since $\dot{V}(t) < 0$. This is observed in our simulations (see Section V) and we also show that the closed-loop eigenvalues have negative real parts for extension. On the other hand, during retraction of the link, the frequency increases and the amplitude of modal variables decreases. However the motion may become unstable since $\dot{V} > 0$. Again this is observed in our numerical simulations and we show that the closed-loop eigenvalues have positive real parts for retraction. The above results are in contrast to those reported by Wang and Wei [10].

V. NUMERICAL RESULTS

In this section, we present the dynamic response of a flexible, spatial, RRP configuration robot (see Fig. 3). The manipulator is assumed to operate in a gravity-free environment, and the prismatic jointed link 3 is considered flexible in the numerical simulation. The flexible link is discretized by two modes in the assumed modes model. The numerical simulation was performed on a SUN-SPARC 10 Workstation. The first-order differential equations of motion (state-space form) with the control input [see (35) and (36)] were solved by a variable step, variable order (of interpolation), predictor-corrector (PECE), Adams algorithm [25]. The desired trajectory for all the joints were generated by using a linear segment with parabolic blends type in time. The joint 1 is commanded to move from $0°$ to $180°$ in 1.0 s, while the joint 2 is commanded to move from $0°$ to $-90°$ during the same time period. The prismatic jointed flexible link, on the other hand, is extended from 0.3 m to 1.0 m in 1.0 s in one case, while it is retracted from 1.0 m to 0.3 m in 1.0 s for the other. The desired joint trajectories are shown in Fig. 4. Table I lists the physical system parameters used for the simulation.

Fig. 5 shows the time history plot of the mode amplitudes of the in-plane and out-of-plane bending vibration components of link 3 during both the extension and retraction of the flexible link 3. We computed the closed-loop eigenvalues of the RRP manipulator system using the Jacobian of the closed-loop equations of motion in state-space form. The closed-loop eigenvalues corresponding to the flexible variables are shown in Figs. 6 and 7. It illustrates the time varying nature of frequencies during motion of the prismatic jointed flexible link 3. It can be observed that real part of the closed-loop eigenvalues of the vibration mode amplitudes become positive, and move into the right-half of the complex plane during retraction of the link 3. This gives rise to unstable response of the flexible variables (see Fig. 5). During extension of the link 3, on the other hand, the real part of the closed-loop eigenvalues of mode variables become negative and move into the left-half of the complex plane, giving rise to stable dynamic response. The time evolution of solutions (β_i) of the clamped-mass frequency equation are illustrated in Fig. 8.

VI. SUMMARY

In this paper, we have presented a discussion on the applicability of using separation of variables and the assumed modes method to discretize a translating flexible beam. We introduced the notion of group velocity for dispersive waves and presented a nondimensionalized Euler–Bernoulli beam equation based on this group velocity for the translating beam. We showed that if the beam is translating at a constant, slow (compared to the group velocity) speed, the principle of separation of variables can be applied. We showed that when the mass and rotary inertia of the load are comparable to that of the flexible beam, the mass end-conditions are more accurate to use for the choice of proper eigen-functions. The clamped-mass boundary conditions, however, lead to a time-dependent frequency equation. We presented a novel method to solve this time-dependent frequency equation by using a differential form of the frequency equation. We then presented a systematic modeling procedure for spatial multi-link flexible manipulators having both revolute and prismatic joints. The assumed modes in conjunction with Lagrangian formulation of dynamics is employed to derive closed form equations of motion. We showed, using a model-based control law which decouples the joint motion from the flexible dynamics, that the closed-loop dynamic response of flexible modal variables become unstable during retraction of a flexible link, compared to the stable dynamic response during extension of the link. The above results were illustrated with numerical simulations of a RRP flexible manipulator.

REFERENCES

[1] W. J. Book, "Recursive lagrangian dynamics of flexible manipulator arms," *Int. J. Robot. Res.*, vol. 3, no. 3, pp. 87–101, 1984.
[2] R. H. Cannon, Jr. and E. Schmitz, "Initial experiments on the end-point control of a flexible one-link robot," *Int. J. Robot. Res.*, vol. 3, no. 3, pp. 62–75, 1984.
[3] P. Chedmail, Y. Aoustin, and C. Chevallereau, "Modeling and control of flexible robots," *Int. J. Numer. Methods Eng.*, vol. 32, pp. 1595–1619, 1991.
[4] A. De Luca and B. Siciliano, "Closed-form dynamic model of planar multilink lightweight robots," *IEEE Trans. Syst. Man, Cybern.*, vol. 21, no. 4, pp. 826–839, 1991.
[5] G. Hastings and W. J. Book, "Verification of a linear dynamic model for flexible robotic manipulators," in *Proc. IEEE Int. Conf. Robotics and Automat.*, 1986, pp. 1024–1029.
[6] C.-J. Li and T. S. Sankar, "Systematic methods for efficient modeling and dynamics computation of flexible robot manipulators," *IEEE Trans. Syst., Man, Cybern.*, vol. 23, no. 1, pp. 77–94, 1993.
[7] K. W. Buffinton, "Dynamics of elastic manipulators with prismatic joints," *ASME J. Dynamic Syst., Meas. Contr.*, vol. 114, pp. 41–49, 1992.
[8] N. G. Chalhoub and A. G. Ulsoy, "Dynamic simulation of a lead-screw driven flexible robot arm and controller," *ASME J. Dynamic Syst., Meas., Contr.*, vol. 108, pp. 119–126, 1986.
[9] K. Krishnamurthy, "Dynamic modeling of a flexible cylindrical manipulator," *J. Sound and Vibration*, vol. 132, no. 1, pp. 143–154, 1989.
[10] P. K. . Wang and J. D. Wei, "Vibrations in a moving flexible robot arm," *J. Sound and Vibration*, vol. 116, no. 1, pp. 149–160, 1987.
[11] J. Yuh and T. Young, "Dynamic modeling of an axially moving beam in rotation: Simulation and experiment," *ASME J. Dynamic Syst., Meas., Contr.*, vol. 113, pp. 34–40, 1991.
[12] K. W. Buffinton and T.R. Kane, "Dynamics of beam moving over supports," *Int. J. Solids Structure*, vol. 21, no. 7, pp. 617–643, 1985.
[13] B. Tabarrok, C. M. Leech, and Y. I. Kim, "On the dynamics of axially moving beams," *J. Franklin Inst.*, vol. 297, no. 3, pp. 201–220, 1974.
[14] S. S. K. Tadikonda and H. Baruh, "Dynamics and control of a translating flexible beam with a prismatic joint," *ASME J. Dynamic Syst., Meas., Contr.*, vol. 114, pp. 422–427, 1992.
[15] A. K. Misra and V. J. Modi, "Deployment and retrieval of shuttle supported tethered satellites," *J. Guidance*, vol. 5, no. 3, pp. 278–285, 1982.
[16] K. Tsuchiya, "Dynamics of a spacecraft during extension of flexible appendages," *J. Guidance*, vol. 6, no. 1, pp. 100–103, 1983.
[17] C. W. Wampler, K. W. Buffinton, and S. H. Jia, "Formulation of equations of motion for systems subject to constraints," *ASME J. Appl. Mech.*, vol. 152, pp. 465–470, 1985.
[18] M. S. Jankovic, "Comments on 'Dynamics of a spacecraft during extension of flexible appendages,'" *J. Guidance*, vol. 7, no. 1, pp. 128, 1983.
[19] R. J. Theodore and A. Ghosal, "Comparison of the assumed modes and finite element models for flexible multi-link manipulators," *Int. J. Robot. Res.*, vol. 14, no. 2, pp. 91–111, 1995.
[20] S. Timoshenko, D. H. Young, and W. Weaver, Jr., *Vibration Problems in Engineering*, 4th ed. New York: Wiley, 1974.
[21] G. B. Whitham, *Linear and Nonlinear Waves*. New York: Wiley, 1974.
[22] K. H. Low, "Solution schemes for the system equations of flexible robots," *J. Robot. Syst.*, vol. 6, no. 4, pp. 383–405, 1989.
[23] H. Asada and J.-J. E. Slotine, *Robot Analysis and Control*. New York: Wiley, 1986.
[24] A. De Luca and B. Siciliano, "Relevance of dynamic models in analysis and synthesis of control laws for flexible manipulators", in *Robotics and Flexible Manufacturing Systems*, J. C. Gentina and S. G. Tzafestas, Eds. Amsterdam, The Netherlands: Elsevier, 1992, pp. 161–168.
[25] L. F. Shampine and M. K. Gordon, *Computer Solution of Ordinary Differential Equations: The Initial Value Problem*. San Francisco, CA: Freeman, 1975.